Data Visualization using Spline Functions

Maria Hussain
Department of Mathematics
Lahore College for Women University, Lahore, Pakistan
mariahussain_1@yahoo.com

Malik Zawwar Hussain
Department of Mathematics
University of the Punjab, Lahore, Pakistan
malikzawwar.math@pu.edu.pk

Muhammad Sarfraz
Department of Information Sciences
Adailiya Campus, Kuwait University, Kuwait
prof.m.sarfraz@gmail.com and sarfraz@cfw.kuniv.edu

Abstract

A two parameter family of C^1 rational cubic spline functions is presented for the graphical representation of shape preserving curve interpolation for shaped data. These parameters have a direct impact on the shape of the curve. Constraints are developed on one family of the parameters to visualize positive, monotone and convex data while other family of parameters can assume any positive values. The problem of visualization of constrained data is also addressed when the data is lying above a straight line and curve is required to lie on the same side of the line. The approximation order of the proposed rational cubic function is also investigated and is found to be $O\left(h_i^3\right)$.

Keywords: Spline, Visualization, Data, Shape, Error analysis.

1. Introduction

Shape control (see Gregory and Sarfraz (1990), Habib and Sakai (2008)), shape design (see Dejdumrong and Tongtar (2007)) and shape preservation (see Sarfraz (2003), Schmidt and Hess (1988), Schultz (1973)) are important areas for graphical presentation of data. In data visualization environment, a user is always interested in graphical representation of the data. Positive, monotone and convex are the basic shapes of data. Rate of dissemination of drugs in blood, population growth (see Butt and Brodlie (1993)) and half-life of a radioactive substance are always positive. Monotonicity is applied in the specification of Digital to Analog Converters (DACs), Analog to Digital Converters (ADCs) and sensors. These devices are used in control system applications where non-monotonicity is unacceptable. Other applications of monotone data are erythrocyte sedimentation rate (E.S.R.) in cancer patients and uric acid level in patients suffering from gout (see Hussain and Hussain (2007)). Convexity has its applications in non-linear programming, designing of telecommunication system, engineering drawing, approximation theory etc. The data arising in an optimization problem may be convex

(Brodlie and Butt (1991)). Due to these applications, development of data visualization schemes which preserve the shape of data, is a germane area of research.

The problem of data visualization of planar data has been discussed by a number of authors. Brodlie and Butt (1991) developed C^1 schemes to preserve the shape of convex data. The same authors in (Brodlie and Butt (1993)) developed a C^1 positivity preserving scheme for 2D data. The authors in (Brodlie and Butt, (1991), (1993)), each interval where the shape of data was lost, divided it into two subintervals by inserting an extra knot in such a way that the shape of data was preserved. The piecewise cubic interpolant was used to interpolate the data over each subinterval. Fahr and Kallay (1992) used a C^1 monotone rational B-spline of degree one to preserve the shape of monotone data. Goodman, Ong and Unsworth (1991) presented two interpolating schemes to visualize the shape of data lying on one side of the straight line using rational cubic function. The first scheme scaled weights by some scale factors and the second scheme adopted the method of insertion of a new interpolation point. Unlike, Butt and Brodlie (1991), (1993), Goodman, Ong and Unsworth (1991), the data visualization schemes for shape preserving curve data developed in this paper neither require the specification of interval in which the shape of data is lost nor scaling of weights. The schemes developed in this paper, assure an automated selection of parameters in each subinterval. Goodman (2002) provided a comprehensive survey of shape preserving interpolating algorithms for planar data. The rational functions used in Hussain and Hussain (2007), Sarfraz, Butt and Hussain (2001), Sarfraz (2003), have two free parameters which are constrained to visualize the shape of data. The data visualization schemes developed in this paper also has two parameters but only one is constrained to visualize the shape preserving curve data. Hussain and Sarfraz used rational cubic function in its most generalized form (four parameters) to preserve the shape of positive and monotone planar data in Hussain and Sarfraz (2008) and Hussain and Sarfraz (2009) respectively. On the other hand the schemes developed in this paper are visualizing the shape preserving curve data by developing constraints on a single parameter. Hence the scheme developed in this paper is computationally economical than Hussain and Hussain (2007), Hussain and Sarfraz (2008), (2009), Sarfraz, Butt and Hussain (2001), Sarfraz (2003). Lamberti and Manni (2001) used cubic Hermite in parametric form to preserve the shape of data. The step length was used as tension parameters to preserve the shape of planar functional data. The first order derivatives at the knots were estimated by a tri-diagonal system of equations which assured C^2 continuity at the knots. The data visualization schemes developed in this paper does not alter the step length to visualize the shape of data. Schmidt and Hess (1988) developed sufficient conditions on derivatives at the knots to assure positivity of interpolating cubic polynomial over the interval thus it is restricted to just data without derivatives, whereas, the schemes developed in this paper are applicable to both data and data with derivatives.

This paper has been devoted to a rational cubic spline scheme for visualization of shaped data. A two parameter family of C^1 rational cubic spline functions has been presented for shape preserving curve interpolation. The two parameter family has a direct impact on the shape of the curve. The data dependent constraints have been developed on one family of the parameters to introduce independent curve schemes to visualize positive, monotone and convex data. However, the other family of parameters has been left as free, it can assume any positive values to further refine the curve schemes if needed. The problem of visualization of constrained data is also addressed when the data is lying above a straight line and curve is required to lie on the same side of the line. Ann error analysis has also been the part of this study. The approximation order of rational cubic spline function has been has been investigated and is found to be $O\left(h_i^3\right)$.

The remainder of the paper is organized as follows. In Section 2, the C^1 rational cubic spline function with two parameters has been introduced. Sections 3 and 4 discuss the problem of shape preservation of positive data and data lying above the straight line respectively. The problems of monotony and convexity preservation of data are discussed in Sections 5 and 6 respectively. Section 7 discusses the error of approximation. Finally, Section 8 concludes the paper.

2. Rational Cubic Spline

Let $\left\{\left(x_i, f_i\right), i = 0,1,2,...,n\right\}$ be the given set of data points defined over the interval $\left[a,b\right]$, where $a = x_0 < x_1 < x_2 < \cdots < x_n = b$. A piecewise rational cubic function with two parameters is defined over each subinterval $I_i = \left[x_i, x_{i+1}\right]$, $i = 0,1,2,...,n-1$ as:

$$S_i\left(x\right) = \frac{A_0\left(1-\theta\right)^3 + A_1\left(1-\theta\right)^2\theta + A_2\left(1-\theta\right)\theta^2 + A_3\theta^3}{1+\left(\alpha_i - \beta_i\right)\left(1-\theta\right)\theta}, \tag{1}$$

where $\theta = \dfrac{x - x_i}{h_i}$. The piecewise rational cubic function (1) will be C^1 if it satisfies the following interpolatory conditions

$$S_i\left(x_i\right) = f_i,\ S_i\left(x_{i+1}\right) = f_{i+1},\ S_i^{(1)}\left(x_i\right) = d_i,\ S_i^{(1)}\left(x_{i+1}\right) = d_{i+1}. \tag{2}$$

$S_i^{(1)}\left(x\right)$ denotes the derivative with respect to x and d_i denotes the derivative values estimated or given. The C^1 continuity conditions defined in (2) asserts the following values of unknowns A_i, $i = 0,1,2,3$:

$$A_0 = f_i,$$
$$A_1 = \left(\left(\alpha_i - \beta_i\right) + 3\right) f_i + h_i d_i,$$
$$A_2 = \left(\left(\alpha_i - \beta_i\right) + 3\right) f_{i+1} - h_i d_{i+1},$$
$$A_3 = f_{i+1}.$$

These values of A_i, $i = 0,1,2,3$ reformulate the rational cubic function (1) to the following C^1 piecewise cubic spline

$$S_i(x) = \frac{p_i(\theta)}{q_i(\theta)}, \tag{3}$$

where

$$p_i(\theta) = f_i(1-\theta)^3 + \left\{\left((\alpha_i - \beta_i) + 3\right) f_i + h_i d_i\right\}(1-\theta)^2 \theta + \left\{\left((\alpha_i - \beta_i) + 3\right) f_{i+1} - h_i d_{i+1}\right\}(1-\theta)\theta^2$$
$$+ f_{i+1}\theta^3,$$
$$q_i(\theta) = 1 + (\alpha_i - \beta_i)(1-\theta)\theta.$$

It is noted when $\alpha_i = \beta_i$, the rational cubic spline (3) reduces to cubic Hermite spline. The parameters α_i and β_i can assume any real value but in this paper, for the ease of manipulation these are assumed positive real number.

2.1 Some Observations

The parameters α_i and β_i involved in the definition rational cubic function have a direct impact on the shape of curve. The mathematical and graphical illustration of this impact is described as:

The increase of either of the parameter α_i and β_i reduces the rational cubic spline to a linear interpolant, which is mathematically expressed as:

$$\lim_{\alpha_i \to \infty} S_i(x) = \lim_{\beta_i \to \infty} S_i(x) = (1-\theta) f_i + \theta f_{i+1}.$$

Same observation is made if we increase both the parameters α_i and β_i simultaneously. To illustrate this impact the rational cubic spline (3) is reformulated as:

$$S_i(x) = f_i(1-\theta) + f_{i+1}\theta + \frac{R}{q_i(\theta)}, \tag{4}$$

where

$$R = (1-\theta)(2\theta-1) h_i \Delta_i - (1-\theta)^2 \theta h_i d_i + (1-\theta)\theta^2 h_i d_{i+1}.$$

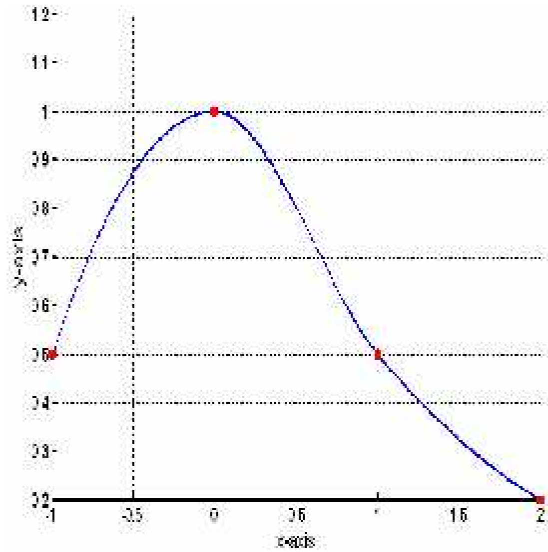

Figure 1. Cubic Hermite spline.

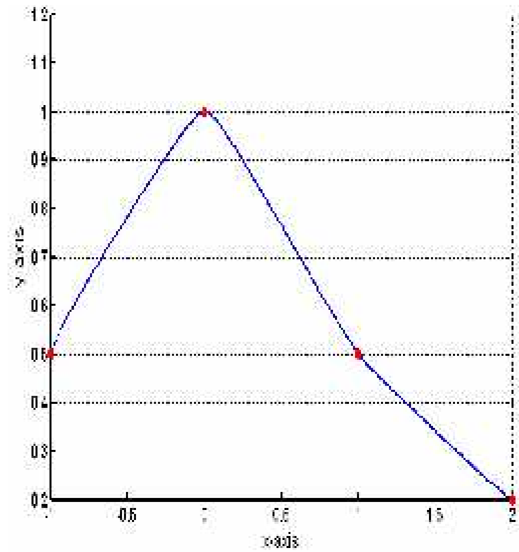

Figure 2. Rational cubic spline ($\alpha_i = 10$, $\beta_i = 0.1$).

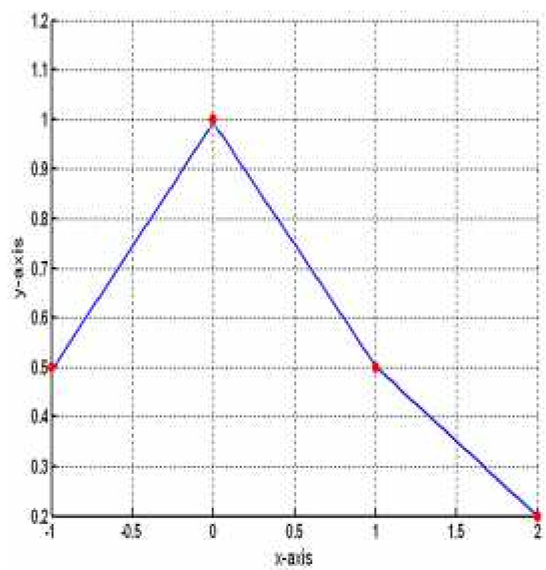

Figure 3. Rational cubic spline ($\alpha_i = 0.1$, $\beta_i = 100$).

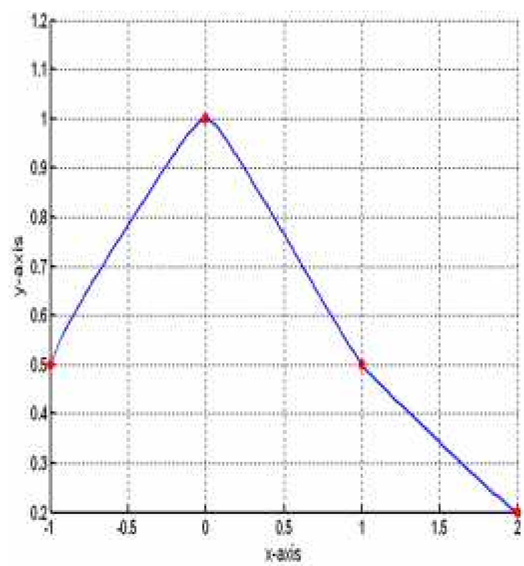

Figure 4. Rational cubic spline ($\alpha_i = 100$, $\beta_i = 90$).

From (4), the following observation is made:

$$\lim_{\alpha_i,\beta_i\to\infty} S_i(x) = \lim_{\alpha_i,\beta_i\to\infty} \left\{ f_i(1-\theta) + f_{i+1}\theta + \frac{R}{q_i(\theta)} \right\} = f_i(1-\theta) + f_{i+1}\theta .$$

Hence, the individual or simultaneous increase of the value of these parameters reduces the rational cubic function (3) in the interval $I_i = [x_i, x_{i+1}]$ to a straight line

$f_i(1-\theta)+f_{i+1}\theta$. These observations are implemented on the data set $\{(x_i, f_i):(-1,0.5),(0,1.0),(1,0.5),(2,0.2)\}$ taken from Hussain and Sarfraz (2009) and demonstrated graphically in Figure 1-4.

3. Positive Curve Data Visualization

Let $\{(x_i, f_i),\ i=0,1,2,...,n\}$ be the positive data defined over the interval $[a,b]$. The necessary condition for the positivity of data is

$$f_i > 0\,,\ i=0,1,2,...,n\,. \tag{5}$$

The piecewise rational cubic spline (3) preserves positivity if

$$S_i(x) > 0\,,\ i=0,1,2,...,n-1\,.$$

$S_i(x) > 0$ if

$$p_i(\theta) > 0 \text{ and } q_i(\theta) > 0\,.$$

$q_i(\theta) > 0$ if

$$\alpha_i > \beta_i\,.$$

Using the result developed by Schmidt and Hess (1988), cubic polynomial $p_i(\theta) > 0$ if

$$\left(p_i'(0),\, p_i'(1)\right) \in R_1 \cup R_2\,,$$

where

$$R_1 = \left\{(a,b) : a > \frac{-3f_i}{h_i},\, b < \frac{3f_{i+1}}{h_i}\right\},$$

$$R_2 = \left\{\begin{array}{l}(a,b):36f_i f_{i+1}\left(a^2+b^2+ab-3\Delta_i(a+b)+3\Delta_i^2\right)+3\left(f_{i+1}a-f_ib\right)\left(2h_iab-3f_{i+1}a+3f_ib\right)\\ \qquad +4h_i\left(f_{i+1}a^3-f_ib^3\right)-h_i^2a^2b^2>0\end{array}\right\}$$

For the rational cubic spline (3), we have

$$p_i'(0) = \frac{(\alpha_i-\beta_i)f_i + h_i d_i}{h_i}\,, \qquad p_i'(1) = \frac{-(\alpha_i-\beta_i)f_{i+1} + h_i d_{i+1}}{h_i}\,.$$

$\left(p_i'(0),\, p_i'(1)\right) \in R_1$ if

$$p_i'(0) > \frac{-3f_i}{h_i}\,,\ p_i'(1) < \frac{3f_{i+1}}{h_i}\,.$$

This leads to the following conditions:

$$\alpha_i > Max\left\{\beta_i - \frac{h_i d_i}{f_i},\, \beta_i + \frac{h_i d_{i+1}}{f_{i+1}}\right\}. \tag{6}$$

Further $\left(p_i'(0), p_i'(1)\right) \in R_2$ if

$$\phi(\alpha_i,\beta_i) = 36 f_i f_{i+1}[\phi_1^2(\alpha_i,\beta_i) + \phi_2^2(\alpha_i,\beta_i) + \phi_1(\alpha_i,\beta_i)\phi_2(\alpha_i,\beta_i) - 3\Delta_i\left(\phi_1(\alpha_i,\beta_i) + \phi_2(\alpha_i,\beta_i)\right) + 3\Delta_i^2]$$
$$+3[f_{i+1}\phi_1(\alpha_i,\beta_i) - f_i\phi_2(\alpha_i,\beta_i)][2h_i\phi_1(\alpha_i,\beta_i)\phi_2(\alpha_i,\beta_i) - 3f_{i+1}\phi_1(\alpha_i,\beta_i) + 3f_i\phi_2(\alpha_i,\beta_i)]$$
$$+4h_i[f_{i+1}\phi_1^3(\alpha_i,\beta_i) - f_i\phi_2^3(\alpha_i,\beta_i)] - h_i^2\phi_1^2(\alpha_i,\beta_i)\phi_2^2(\alpha_i,\beta_i) \geq 0, \tag{7}$$

with $\phi_1(\alpha_i,\beta_i) = p_i'(0)$ and $\phi_2(\alpha_i,\beta_i) = p_i'(1)$.

Positivity of $p_i(\theta)$ can be assured from either (6) or (7), but the simplicity of computation in (6) justify it as a rational choice. The whole discussion can be summarized as follows:

Theorem 3.1. The piecewise rational cubic interpolant $S(x)$, defined over the interval $[a,b]$, in (3), is positive if in each sub interval $I_i = [x_i, x_{i+1}]$ the following sufficient conditions are satisfied

$$\beta_i > 0,$$
$$\alpha_i > Max\left\{\beta_i, \beta_i - \frac{h_i d_i}{f_i}, \beta_i + \frac{h_i d_{i+1}}{f_{i+1}}\right\}.$$

The above constraints can be rearranged as:

$$\beta_i > 0,$$
$$\alpha_i = l_i + Max\left\{\beta_i, \beta_i - \frac{h_i d_i}{f_i}, \beta_i + \frac{h_i d_{i+1}}{f_{i+1}}\right\},\ l_i > 0.$$

3.1 Demonstration

In this Section we shall illustrate the positivity preserving scheme developed in Section 3 through numerical examples.

Example 3.1. Consider the positive data set of Hussain and Sarfraz (2008) shown in Table 1. Figure 5 is produced from the positive data in Table 1 using cubic Hermite spline which looses the shape of data. Positive curve in Figure 6 is produced from the positive data set in Table 1 using the positive data visualization scheme developed in Section 3. The values of derivatives and parameters are provided in Table 2.

Table 1. Positive data set.

x	1	2	3	8	10	11	12	14
f	14	8	2	0.8	0.5	0.25	0.40	0.37

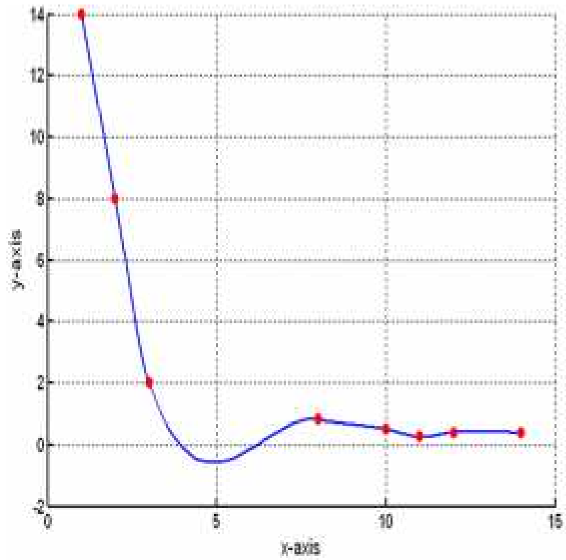

Figure 5. Cubic Hermite spline.

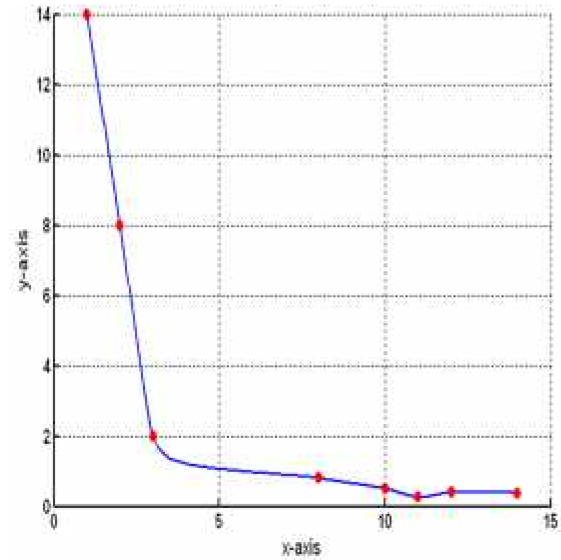

Figure 6. Positive rational cubic spline.

Table 2. Numerical results for Figure 6.

i	1	2	3	4	5	6	7	8
d_i	-6.0	-6.0	-3.12	-0.195	-0.2	-0.05	- 0.0675	- 0.1250
α_i	3.5	3.02	15.3125	4.1333	2.5	1.95	9.8333	-
β_i	0.5	0.5	0.5	0.5	0.5	0.5	0.5	-

Example 3.2. Another positive data set is considered in Table 3. The negative curve in Figure 7 through positive data taken in Table 3 is produced using cubic Hermite spline which looses the shape of data. The curve in Figure 8 is produced through positive data in Table 3 using the scheme developed in Section 3. It is seen that the positive shape of the data is preserved. Figure 9 and Figure 10 provides the clooser view of Figure 8.

Table 3. Positive data set.

x	-3	-2	-1	0	1	2	3
f	0.0488	0.2353	2.0000	4.0000	2.0000	0.2353	0.0488

Table 4. Numerical results for Figure 8.

i	1	2	3	4	5	6	7
d_i	-0.6026	0.9756	1.8824	0	-1.8824	-0.9756	0.6026
α_i	5.2331	1.6255	0.9432	0.9432	1.6215	5.2331	-
β_i	0.0010	0.0010	0.0010	0.0010	0.0010	0.0010	-

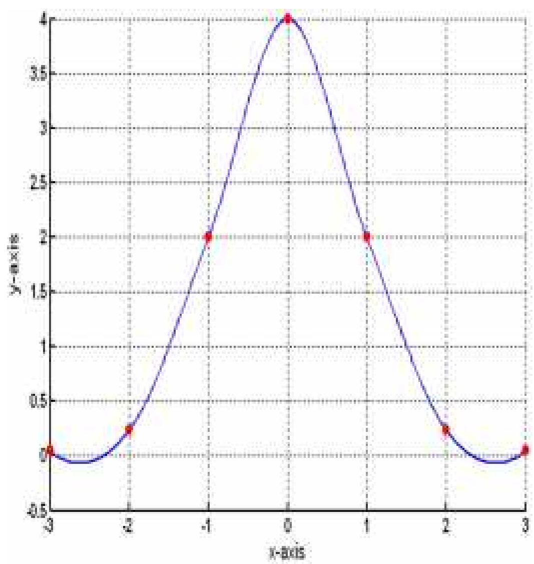

Figure 7. Cubic Hermite spline.

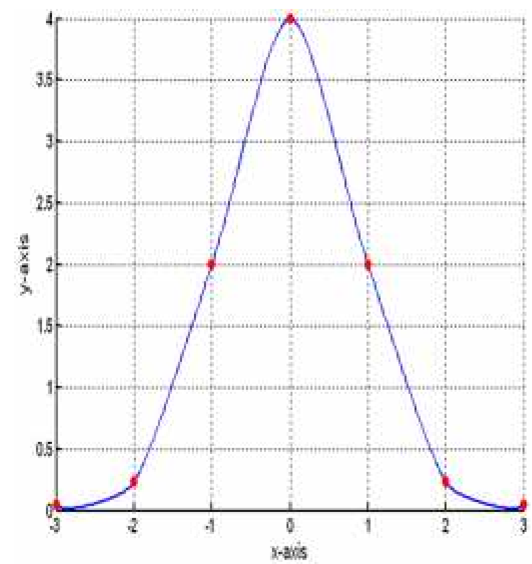

Figure 8. Positive rational cubic spline.

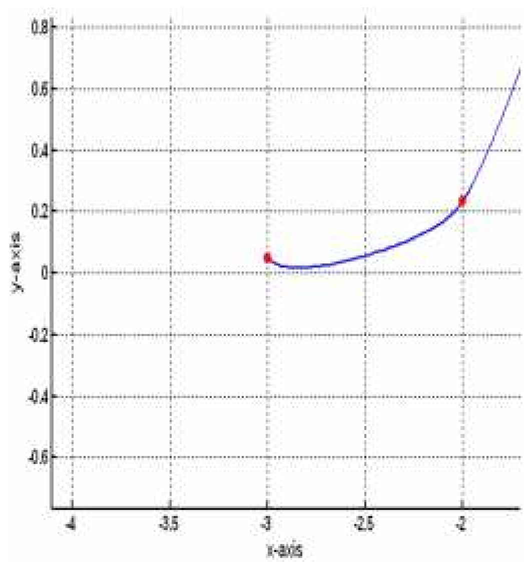

Figure 9. Closer view of Figure 8.

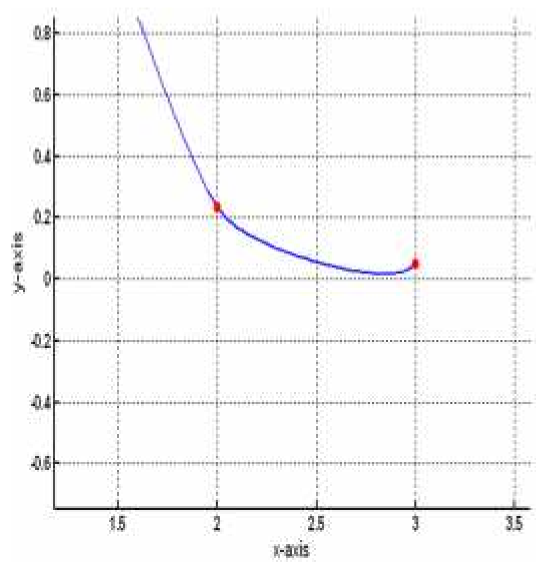

Figure 10. Closer view of Figure 8.

4. Constrained Curve Data Visualization

Let $\{(x_i, f_i),\ i = 0,1,2,...,n\}$ be the given set of data points lying above the straight line $y = mx + c$ i.e.

$$f_i > mx_i + c\,,\ \ \forall\ \ i = 0,1,2,...,n\,. \tag{8}$$

The curve will lie above the straight line if the rational cubic function (3) satisfies the following condition

$$S(x) > mx + c\,,\ \forall\ \ x \in [x_0, x_n]\,.$$

For each subinterval $I_i = [x_i, x_{i+1}]$, the above relation can be expressed as

$$S_i(x) = \frac{p_i(\theta)}{q_i(\theta)} > a_i(1-\theta) + b_i\theta\,, \tag{9}$$

where $a_i(1-\theta) + b_i\theta$ is the parametric equation of straight line with $a_i = mx_i + c$ and $b_i = mx_{i+1} + c$. Multiplying both sides of (9) with $q_i(\theta)$ assuming that $\alpha_i > \beta_i$ and after some rearrangement, (9) reduces to

$$U_i(\theta) = \sum_{i=0}^{3} (1-\theta)^{3-i}\,\theta^i B_i\,,$$

where

$$B_0 = f_i - a_i\,,$$
$$B_1 = \big((\alpha_i - \beta_i) + 3\big) f_i + h_i d_i - b_i - 2a_i - (\alpha_i - \beta_i) a_i\,,$$
$$B_2 = \big((\alpha_i - \beta_i) + 3\big) f_{i+1} - h_i d_{i+1} - 2b_i - a_i - (\alpha_i - \beta_i) b_i\,,$$
$$B_3 = f_{i+1} - b_i\,.$$

$$U_i(\theta) > 0 \ \text{ if } \ B_i > 0\,,\ i = 0,1,2,3.$$

We know that $B_0 > 0$ and $B_3 > 0$ are true from the necessary condition (8).

Now, $B_1 > 0$ if

$$\alpha_i > \beta_i + \frac{(-f_i - h_i d_i + b_i)}{f_i - a_i}\,.$$

Similarly, $B_2 > 0$ if

$$\alpha_i > \beta_i + \frac{(-f_{i+1} + h_i d_{i+1} + a_i)}{f_{i+1} - b_i}\,.$$

The above discussion can be summarized as follows:

Theorem 4.1. The piecewise rational cubic interpolant $S(x)$, defined over the interval $[a,b]$, in (3), preserves the shape of data that lies above the straight line if in each subinterval $I_i = [x_i, x_{i+1}]$ the following sufficient conditions are satisfied

$$\beta_i > 0,$$

$$\alpha_i > Max\left\{ \beta_i, \beta_i + \frac{(-f_i - h_i d_i + b_i)}{f_i - a_i}, \beta_i + \frac{(-f_{i+1} + h_i d_{i+1} + a_i)}{f_{i+1} - b_i} \right\}.$$

The above constraints can be rearranged as:

$$\beta_i > 0,$$

$$\alpha_i = m_i + Max\left\{ \beta_i, \beta_i + \frac{(-f_i - h_i d_i + b_i)}{f_i - a_i}, \beta_i + \frac{(-f_{i+1} + h_i d_{i+1} + a_i)}{f_{i+1} - b_i} \right\},\ m_i > 0.$$

4.1 Demonstration

In this Section we shall illustrate the constrained data preserving scheme developed in Section 4 through numerical examples.

Example 4.1. Consider the positive data set of Hussain and Sarfraz (2008) shown in Table 5. This data set is lying above the straight line $y = \frac{x}{2} + 1$. Figure 11 is produced from the data set in Table 5 using cubic Hermite spline which looses the shape of data. Figure 12 is produced from the data set in Table 5 using data visualization scheme developed in Section 4. It is observable from the Figure 12 that the curve is lying above the straight line $y = \frac{x}{2} + 1$.

Table 5. Positive data set above the line $y = \frac{x}{2} + 1$.

x	2	3	7	8	10	13	14
f	12	4.5	6.5	10	6.3	12	18

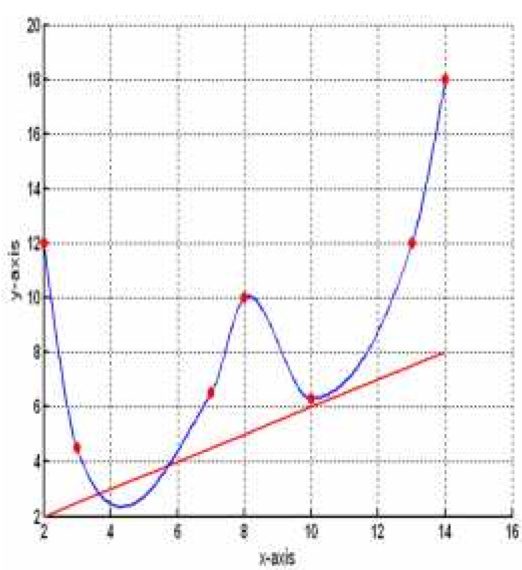

Figure 11. Cubic Hermite spline.

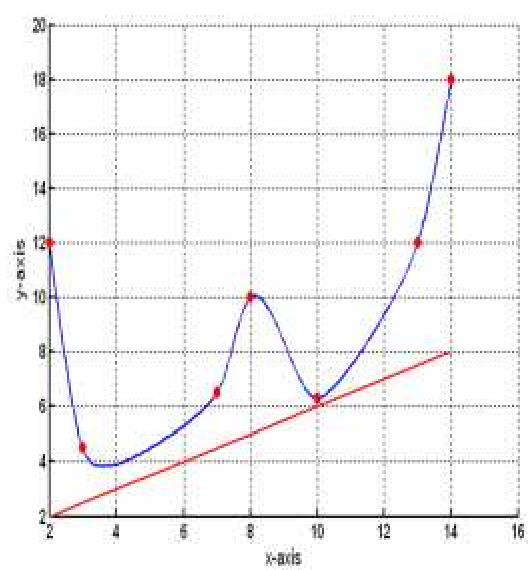

Figure 12. Constrained rational cubic spline.

Table 6. Numerical results for Figure 12.

i	1	2	3	4	5	6	7
d_i	-9.1000	-3.5000	2.0000	0.8250	0.0250	3.9500	7.0250
α_i	1.0000	1.0000	1.0000	1.0000	4.7500	1.0000	-
β_i	0.0010	0.0010	0.0010	0.0010	0.0010	0.0010	-

Example 4.2. Consider another positive data set of Kvasov (2000) shown in Table 7. This data set is lying above the straight line $y = \frac{x}{2} + 1$. Figure 13 is produced from the data set in Table 7 using cubic Hermite spline which looses the shape of data. Curve lying above the straight line $y = \frac{x}{2} + 1$, in Figure 14, is produced from the data visualization scheme developed in Section 4.

Table 7. Positive data set above the line $y = \frac{x}{2} + 1$.

x	0	2	3	5	6	8	11	14	15
f	6.5	6.5	6.5	6.5	6.5	16	50	60	85

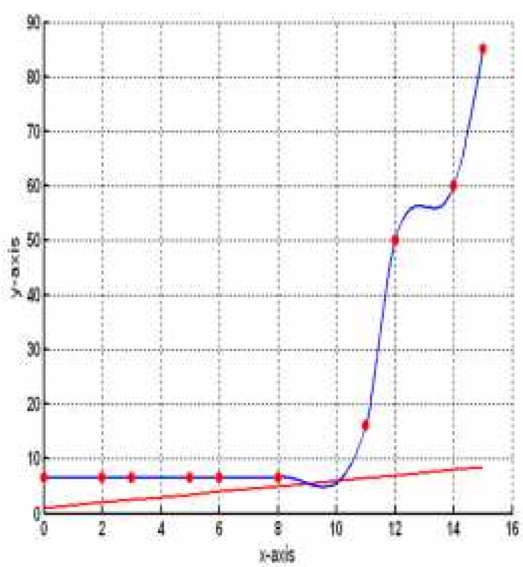

Figure 13. Cubic Hermite spline.

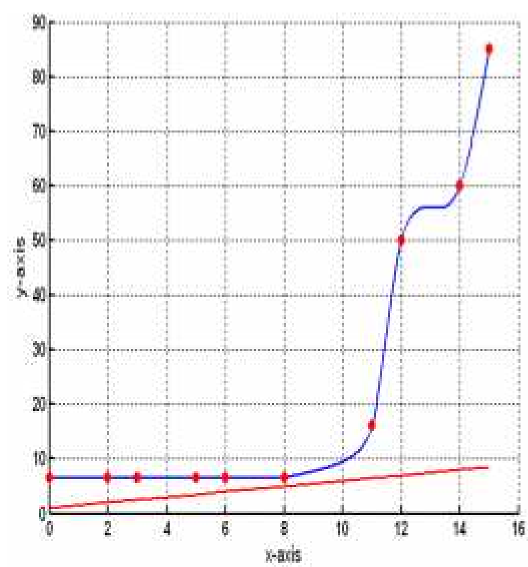

Figure 14. Constrained rational cubic spline.

Table 8. Numerical results for Figure 14.

i	1	2	3	4	5	6	7	8	9	10
d_i	0	0	0	0	0	1.5833	18.5833	19.5000	15.0	31.6667
α_i	1.0	1.0	1.0	1.0	1.4444	5.7105	1.0000	1.0000	1.0	-
β_i	0.5	0.5	0.5	0.5	0.5000	0.5000	0.5000	0.5000	0.5	-

5. Monotone Curve Data Visualization

Let $\{(x_i, f_i),\ i = 0,1,2,...,n\}$ be the monotone data defined over the interval $[a,b]$ such that

$$f_i < f_{i+1},\ \Delta_i = \frac{f_{i+1} - f_i}{h_i} > 0,\ d_i > 0,\ i = 0,1,2,...,n-1. \tag{10}$$

The piecewise rational cubic function (3) preserves monotony if

$$S_i^{(1)}(x) > 0,\ i = 0,1,2,...,n-1,$$

where

$$S_i^{(1)}(x) = \frac{\sum_{i=0}^{4} (1-\theta)^{4-i} \theta^i C_i}{(q_i(\theta))^2}, \tag{11}$$

$$C_0 = d_i,$$
$$C_1 = (2(\alpha_i - \beta_i) + 6)\Delta_i - 2d_{i+1},$$
$$C_2 = 3\Delta_i + ((\alpha_i - \beta_i) + 3)\{((\alpha_i - \beta_i) + 3)\Delta_i - d_{i+1} - d_i\},$$
$$C_3 = (2(\alpha_i - \beta_i) + 6)\Delta_i - 2d_i,$$
$$C_4 = d_{i+1}.$$

From (11), $S_i^{(1)}(x) > 0$ if $C_i > 0$, $i = 0,1,2,3,4$. Obviously, $C_0 > 0$ and $C_4 > 0$ are always true from the necessary condition of monotonicity (10). Now, $C_1 > 0$ if

$$\alpha_i > \beta_i + \frac{d_{i+1}}{\Delta_i}.$$

Similarly, $C_2 > 0$ if

$$\alpha_i > \beta_i,$$
$$\alpha_i > \beta_i + \frac{d_i + d_{i+1}}{\Delta_i}.$$

and $C_3 > 0$ if

$$\alpha_i > \beta_i + \frac{d_i}{\Delta_i}.$$

The above can be summarized as:

Theorem 5.1. The piecewise rational cubic interpolant $S(x)$, defined over the interval $[a,b]$, in (3), is monotone if in each subinterval $I_i = [x_i, x_{i+1}]$ the following sufficient conditions are satisfied

$$\beta_i > 0,$$

$$\alpha_i > Max\left\{ \beta_i + \frac{d_i}{\Delta_i},\ \beta_i + \frac{d_{i+1}}{\Delta_i}, \beta_i + \frac{d_i + d_{i+1}}{\Delta_i} \right\}.$$

The above constraints can be rearranged as:

$$\beta_i > 0,$$

$$\alpha_i = n_i + Max\left\{ \beta_i + \frac{d_i}{\Delta_i},\ \beta_i + \frac{d_{i+1}}{\Delta_i}, \beta_i + \frac{d_i + d_{i+1}}{\Delta_i} \right\},\ n_i > 0.$$

5.1 Demonstration

In this Section we shall illustrate the monotone data preserving scheme developed in Section 5 through numerical examples.

Example 5.1. Consider a monotone data set taken in Table 9. Non-monotone curve in Figure 15 from the monotone of Table 9 is produced using cubic Hermite. The monotone curve (from the same data set) is produced in Figure 16 using data visualization scheme developed in Section 4. The values of derivatives at the knots and parameters are provided in Table 10.

Table 9. A monotone data set.

x	8.7	9.2	10	12	15
f	0.1691	0.4694	0.9437	0.9986	0.9999

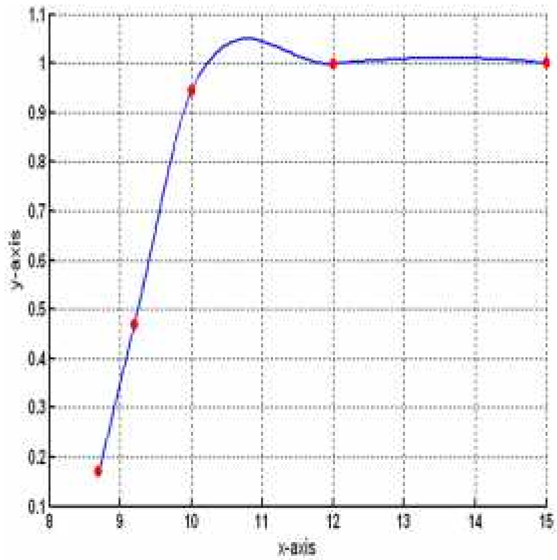

Figure 15. Cubic Hermite spline.

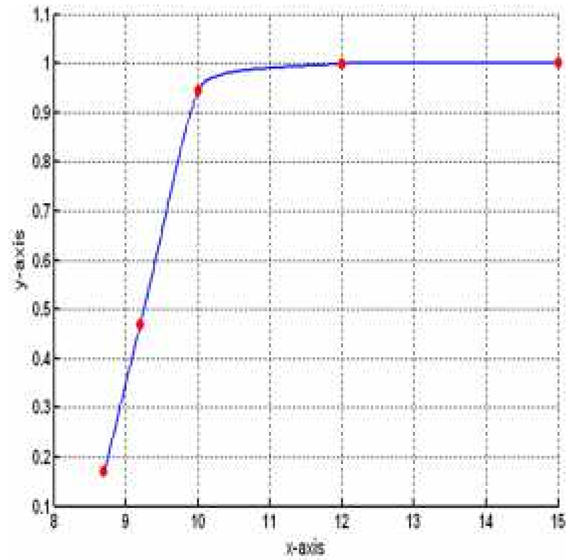

Figure 16. Monotone rational cubic spline.

Table 10. Numerical results for Figure 16.

i	1	2	3	4	5
d_i	0.6036	0.5967	0.3102	0.0139	0.0000
α_i	2.0185	1.5497	11.8271	32.1931	-
β_i	0.0100	0.0100	0.0100	0.0100	-

Example 5.2. Consider another monotone data set shown in Table 11. This data has been taken from Kvasov (2000) with slight modification. Figure 17 is produced from the data set in Table 11 using cubic Hermite spline which looses the monotone shape of data. The monotone curve in Figure 18 is produced using the monotone data visualization scheme developed in Section 5. Its numerical results are shown in Table 12.

Table 11. Monotone data set.

x	0	2	3	5	6	8	9	11	12	14	15
f	10.01	10.02	10.03	10.04	10.05	10.06	10.5	15	50	60	85

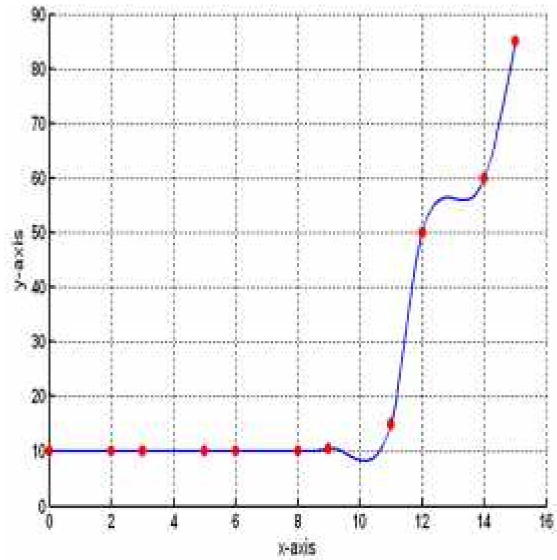

Figure 17. Cubic Hermite spline.

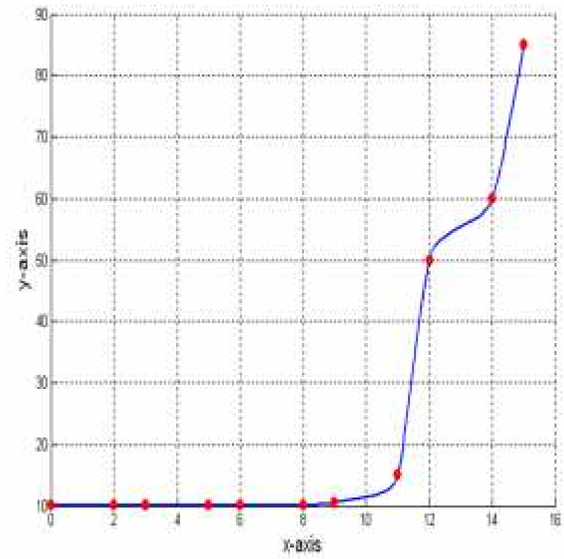

Figure 18. Monotone rational cubic spline.

Table 12. Numerical results for Figure 18.

i	1	2	3	4	5	6	7	8	9	10	11
d_i	0.00 17	0.00 75	0.00 75	0.00 75	0.00 75	0.22 25	1.34 50	18.62 50	20.00 00	15.00 00	31.66 67
α_i	1.83 53	1.50 20	3.00 20	1.50 20	46.00 20	3.56 45	8.87 76	1.10 56	7.00 20	1.86 87	-
β_i	0.00 10	0.00 10	0.00 10	0.00 10	0.00 10	0.00 10	0.00 10	0.00 10	0.00 10	0.00 10	-

6. Convex Curve Data Visualization

Let $\{(x_i, f_i), i = 0,1,2,...,n\}$ be the convex data defined over the interval $[a,b]$ such that

$$\Delta_i < \Delta_{i+1},\ d_i < d_{i+1},\ d_i < \Delta_i < d_{i+1},\ i = 0,1,2,...,n-1 .$$

The piecewise rational cubic function (3) preserves convexity if

$$S_i^{(2)}(x) > 0,\ i = 0,1,2,...,n-1,$$

where

$$S_i^{(2)}(x) = \frac{\sum_{i=0}^{5}(1-\theta)^{5-i}\theta^i D_i}{h_i\left(q_i(\theta)\right)^3}, \tag{12}$$

where

$$D_0 = \left(2(\alpha_i - \beta_i) + 4\right)(\Delta_i - d_i) + 2(\Delta_i - d_{i+1}),$$
$$D_1 = 4(\alpha_i - \beta_i)(\Delta_i - d_i) + 14(\Delta_i - d_i) + 4(\Delta_i - d_{i+1}),$$

$D_2 = 2(\alpha_i - \beta_i)(\Delta_i - d_i) + 12(\Delta_i - d_i) + 4(d_{i+1} - d_i),$
$D_3 = 2(\alpha_i - \beta_i)(d_{i+1} - \Delta_i) + 12(d_{i+1} - \Delta_i) + 4(d_{i+1} - d_i),$
$D_4 = 4(\alpha_i - \beta_i)(d_{i+1} - \Delta_i) + 14(d_{i+1} - \Delta_i) + 4(d_i - \Delta_i),$
$D_5 = (2(\alpha_i - \beta_i) + 4)(d_{i+1} - \Delta_i) + 2(d_i - \Delta_i).$

$S_i^{(2)}(x) > 0$ if

$$(q_i(\theta))^3 > 0,\ D_i > 0,\ i = 0,1,2,3,4,5.$$

$(q_i(\theta))^3 > 0$ if

$$\alpha_i > \beta_i.$$

$D_i > 0,\ i = 0,1,2,3,4,5$ if

$$\beta_i > 0,$$
$$\alpha_i > Max\left\{\beta_i + \frac{(d_{i+1} - \Delta_i)}{\Delta_i - d_i},\ \beta_i + \frac{(\Delta_i - d_i)}{d_{i+1} - \Delta_i}\right\}.$$

The above can be summarized as:

Theorem 6.1. The piecewise rational cubic interpolant $S(x)$, defined over the interval $[a,b]$, in (3), is convex if the following sufficient conditions are satisfied

$$\beta_i > 0,$$
$$\alpha_i > Max\left\{\beta_i + \frac{(d_{i+1} - \Delta_i)}{\Delta_i - d_i},\ \beta_i + \frac{(\Delta_i - d_i)}{d_{i+1} - \Delta_i}\right\}.$$

The above constraints can be rearranged as:

$$\beta_i > 0,$$
$$\alpha_i > Max\left\{\beta_i + \frac{(d_{i+1} - \Delta_i)}{\Delta_i - d_i},\ \beta_i + \frac{(\Delta_i - d_i)}{d_{i+1} - \Delta_i}\right\}.$$

6.1 Demonstration

In this Section we shall illustrate the convex data preserving scheme developed in Section 6 through numerical examples.

Example 6.1. Consider a convex data set taken in Table 13. Figure 19 is produced from the convex data set in Table 13 using cubic Hermite spline which looses the shape of data. Figure 20 is produced from the same data set using the convex data visualization scheme developed in Section 6. It is seen in Figure 20 that the convex shape of data is preserved. The values of derivatives at knots and parameters in the interval are provided in Table 14.

Table 13. A convex data set.

x	2	2.5	3.5	5.5	6
f	-2.5	-4.5	-5.0	-4.5	-1.5

Table 14. Numerical results for Figure 20.

i	1	2	3	4	5
d_i	-5.1667	-2.2500	-0.1250	3.1250	7.1500
α_i	1.7000	4.8667	7.8667	2.7000	-
β_i	0.1000	0.1000	0.1000	0.1000	-

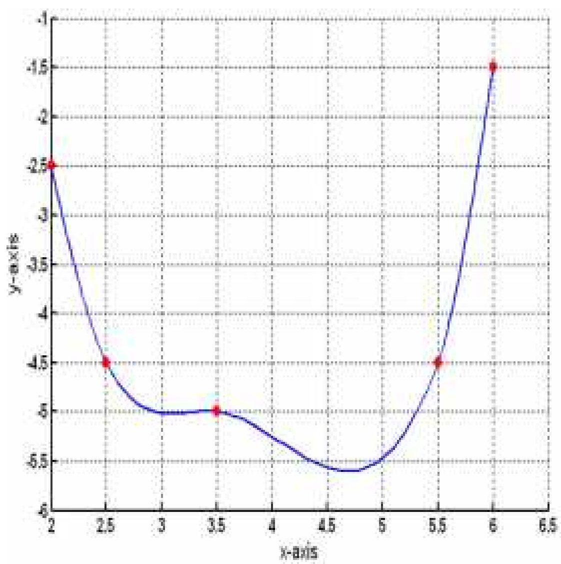

Figure 19. Cubic Hermite spline.

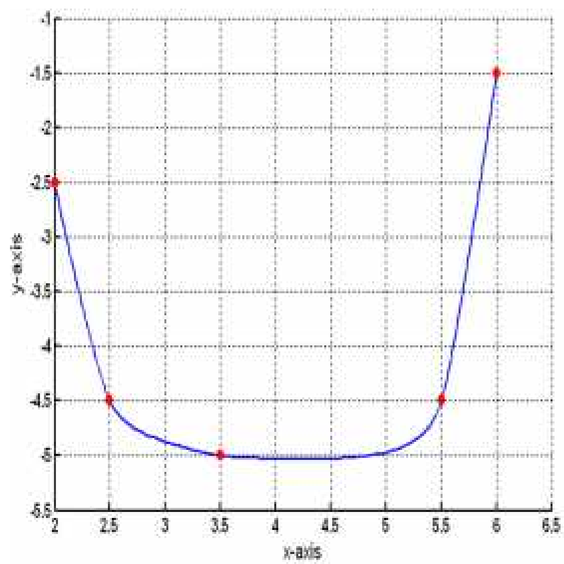

Figure 20. Convex rational cubic spline.

Example 6.2. Consider another convex data set shown in Table 15. This data has been taken from Yahaya, Hussain and Ali (2006). Figure 21 is produced from the convex data set in Table 15 using cubic Hermite spline which looses the shape of data. The convex curve in Figure 22 is produced using convex data visualization scheme developed in Section 6.

Table 15. Convex data set.

x	1	2	4	5	10
f	10.0000	2.5000	0.6250	0.4000	0.1000

Table 16. Numerical results of Figure 22.

i	1	2	3	4	5
d_i	-9.6875	-4.2188	-0.5813	-0.1425	0.0775
α_i	1.5002	9.2107	4.3184	1.6669	-
β_i	0.0001	0.0001	0.0001	0.0001	-

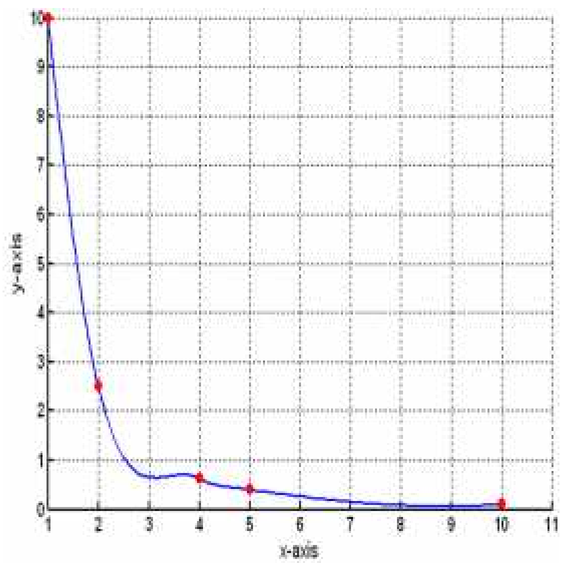

Figure 21. Cubic Hermite spline.

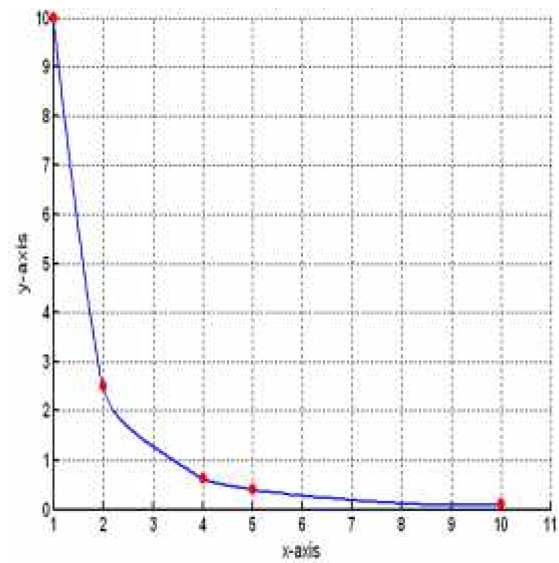

Figure 22. Convex rational cubic spline.

7. Error Estimation of Interpolation

In this Section, the error of interpolation is estimated when the function being interpolated is $f(x) \in C^3[x_0, x_n]$, using the rational cubic function (3). Keeping in view the locality of interpolation scheme developed in Section 2, the error is investigated in an arbitrary subinterval $I_i = [x_i, x_{i+1}]$. The Peano Kernel Theorem (see Schultz (1973)) is used to estimate the error adopting the approach of Duan et al. (2007).

The error in each subinterval $I_i = [x_i, x_{i+1}]$ is defined as:

$$R[f] = f(x) - S_i(x) = \frac{1}{2}\int_{x_i}^{x_{i+1}} f^{(3)}(\tau) R_x\left[(x-\tau)_+^2\right] d\tau . \tag{13}$$

The absolute value of the error in each subinterval is:

$$\left|f(x) - S_i(x)\right| \le \frac{1}{2}\left\|f^{(3)}(\tau)\right\| \int_{x_i}^{x_{i+1}} \left|R_x\left[(x-\tau)_+^2\right]\right| d\tau , \tag{14}$$

where

$$R_x\left[(x-\tau)_+^2\right]=\begin{cases} r(\tau,x), & x_i<\tau<x, \\ s(\tau,x), & x<\tau<x_{i+1}. \end{cases} \tag{15}$$

The $R_x\left[(x-\tau)_+^2\right]$ is the Peano-Kernel. Using (15), $\int_{x_i}^{x_{i+1}}\left|R_x\left[(x-\tau)_+^2\right]\right|d\tau$ can be expressed as:

$$\int_{x_i}^{x_{i+1}}\left|R_x\left[(x-\tau)_+^2\right]\right|d\tau=\int_{x_i}^{x}\left|r(\tau,x)\right|d\tau+\int_{x}^{x_{i+1}}\left|s(\tau,x)\right|d\tau . \tag{16}$$

For the rational cubic function (3), $r(\tau,x)$ and $s(\tau,x)$ have the value

$$r(\tau,x)=(x-\tau)^2-\frac{1}{q_i(\theta)}\left[(x_{i+1}-\tau)^2\left\{(1-\theta)\theta^2(\alpha_i-\beta_i+3)+\theta^3\right\}-2h_i(x_{i+1}-\tau)(1-\theta)\theta^2\right], \tag{17}$$

$$s(\tau,x)=-\frac{1}{q_i(\theta)}\left[(x_{i+1}-\tau)^2\left\{(1-\theta)\theta^2(\alpha_i-\beta_i+3)+\theta^3\right\}-2h_i(x_{i+1}-\tau)(1-\theta)\theta^2\right]. \tag{18}$$

The roots of $r(x,x)$ in $[0,1]$ are $\theta=0$, $\theta=1$ and $\theta^*=\dfrac{\alpha_i-\beta_i+1}{\alpha_i-\beta_i+2}$.

The roots of $r(\tau,x)=0$ are

$$\tau_j=x-\frac{h_i\theta\left(G+(-1)^{j+1}H\right)}{1+(\alpha_i-\beta_i+2)\theta},\ j=1,2,$$

where

$$G=\theta(\alpha_i-\beta_i+2),$$

$$H=\sqrt{(\alpha_i-\beta_i+1)+\theta(\alpha_i-\beta_i)(\alpha_i-\beta_i+2)}.$$

The root of $s(\tau,x)=0$ are $\tau_3=x_{i+1}-\dfrac{2h_i(1-\theta)}{(\alpha_i-\beta_i+2)(1-\theta)+1}$, $\tau_4=x_{i+1}$.

Now, we have the following cases:

Case 1: For $0<\theta<\theta^*$ and $1-H>0$, (14) takes the form

$$\left|f(x)-S_i(x)\right|\le\frac{1}{2}\left\|f^{(3)}(\tau)\right\|h_i^3\omega_1(\alpha_i,\beta_i,\theta),$$

$$\omega_1(\alpha_i,\beta_i,\theta)=\int_{x_i}^{x}\left|r(\tau,x)\right|d\tau+\int_{x}^{x_{i+1}}\left|s(\tau,x)\right|d\tau$$

$$=\int_{x_i}^{\tau_1}r(\tau,x)d\tau-\int_{\tau_1}^{x}r(\tau,x)d\tau-\int_{x}^{\tau_3}s(\tau,x)d\tau+\int_{\tau_3}^{x_{i+1}}s(\tau,x)d\tau$$

$$=\frac{-2\theta^3(G+H)^3}{3\left(1+\theta(\alpha_i-\beta_i+2)\right)^3}+\frac{2\theta^2}{3q_i(\theta)}\left[\frac{-3(1-\theta)\left\{1+\theta(\alpha_i-\beta_i+1)+\theta H\right\}^2}{\left(1+\theta(\alpha_i-\beta_i+2)\right)^2}\right.$$
$$\left.+\frac{\left\{(\alpha_i-\beta_i+3)+\theta(\beta_i-\alpha_i-2)\right\}\left\{1+\theta(\alpha_i-\beta_i+1)+\theta H\right\}^3}{\left(1+\theta(\alpha_i-\beta_i+2)\right)^3}\right]+\frac{\theta^3}{3}$$
$$-\frac{\theta^2\left\{(\beta_i-\alpha_i+1)\theta+(\alpha_i-\beta_i)\right\}}{3q_i(\theta)}+\frac{8(1-\theta)^3\theta^2}{3q_i(\theta)\left\{(\alpha_i-\beta_i+2)(1-\theta)+1\right\}^2}.$$

Case 2: For $0<\theta<\theta^*$ and $1-H<0$, (14) takes the form

$$\left|f(x)-S_i(x)\right|\le\frac{1}{2}\left\|f^{(3)}(\tau)\right\|h_i^3\omega_2(\alpha_i,\beta_i,\theta),$$
$$\omega_2(\alpha_i,\beta_i,\theta)=\int_{x_i}^{x}\left|r(\tau,x)\right|d\tau+\int_{x}^{x_{i+1}}\left|s(\tau,x)\right|d\tau$$
$$=-\int_{x_i}^{t}r(\tau,x)\,d\tau-\int_{x}^{\tau_3}s(\tau,x)\,d\tau+\int_{\tau_3}^{x_{i+1}}s(\tau,x)\,d\tau$$
$$=-\frac{\theta^3}{3}+\frac{\theta^2\left\{(\beta_i-\alpha_i+1)\theta+(\alpha_i-\beta_i)\right\}}{3q_i(\theta)}+\frac{8(1-\theta)^3\theta^2}{3q_i(\theta)\left\{(\alpha_i-\beta_i+2)(1-\theta)+1\right\}^2}.$$

Case 3: For $\theta^*<\theta<1$ and $1-H>0$, (14) takes the form

$$\left|f(x)-S_i(x)\right|\le\frac{1}{2}\left\|f^{(3)}(\tau)\right\|h_i^3\omega_3(\alpha_i,\beta_i,\theta),$$
$$\omega_3(\alpha_i,\beta_i,\theta)=\int_{x_i}^{x}\left|r(\tau,x)\right|d\tau+\int_{x}^{x_{i+1}}\left|s(\tau,x)\right|d\tau$$
$$=\int_{x_i}^{\tau_1}r(\tau,x)\,d\tau-\int_{\tau_1}^{\tau_2}r(\tau,x)\,d\tau+\int_{\tau_2}^{t}r(\tau,x)\,d\tau+\int_{t}^{x_{i+1}}s(\tau,x)\,d\tau$$
$$=\frac{\theta^3}{3}-\frac{\theta^2\left\{(-\alpha_i+\beta_i+1)\theta+(\alpha_i-\beta_i)\right\}}{3q_i(\theta)}\frac{-2\theta^3(G+H)^3}{3\left(1+\theta(\alpha_i-\beta_i+2)\right)^3}$$
$$+\frac{2\theta^2}{3q_i(\theta)}\left[\frac{\left\{(\alpha_i-\beta_i+3)+\theta(\beta_i-\alpha_i-2)\right\}\left\{1+\theta(\alpha_i-\beta_i+1)+\theta H\right\}^3}{\left(1+\theta(\alpha_i-\beta_i+2)\right)^3}\right.$$
$$\left.-\frac{3(1-\theta)\left\{1+\theta(\alpha_i-\beta_i+1)+\theta H\right\}^2}{\left(1+\theta(\alpha_i-\beta_i+2)\right)^2}\right]+\frac{2\theta^3(G-H)^3}{3\left(1+\theta(\alpha_i-\beta_i+2)\right)^3}$$
$$-\frac{2\theta^2}{3q_i(\theta)}\left[\frac{\left\{(\alpha_i-\beta_i+3)+\theta(\beta_i-\alpha_i-2)\right\}\left\{1+\theta(\alpha_i-\beta_i+1)-\theta H\right\}^3}{\left(1+\theta(\alpha_i-\beta_i+2)\right)^3}\right.$$

$$-\frac{3(1-\theta)\{1+\theta(\alpha_i-\beta_i+1)-\theta H\}^2}{\left(1+\theta(\alpha_i-\beta_i+2)\right)^2}\Bigg].$$

Case 4: For $\theta^* < \theta < 1$ and $1-H<0$, (14) takes the form

$$\left|f(x)-S_i(x)\right| \le \frac{1}{2}\left\|f^{(3)}(\tau)\right\| h_i^3 \omega_4(\alpha_i,\beta_i,\theta),$$

$$\begin{aligned}
\omega_4(\alpha_i,\beta_i,\theta) &= \int_{x_i}^{x}\left|r(\tau,x)\right|d\tau + \int_{x}^{x_{i+1}}\left|s(\tau,x)\right|d\tau \\
&= -\int_{x_i}^{\tau_2} r(\tau,x)\,d\tau + \int_{\tau_2}^{t} r(\tau,x)\,d\tau + \int_{t}^{x_{i+1}} s(\tau,x)\,d\tau \\
&= -\frac{\theta^3}{3} + \frac{\theta^2\{(-\alpha_i+\beta_i-1)\theta+(\alpha_i-\beta_i)\}}{3q_i(\theta)} + \frac{2\theta^3(G-H)^3}{3\left(1+\theta(\alpha_i-\beta_i+2)\right)^3} \\
&\quad -\frac{2\theta^2}{3q_i(\theta)}\left[\frac{\{(\alpha_i-\beta_i+3)+\theta(\beta_i-\alpha_i-2)\}\{1+\theta(\alpha_i-\beta_i+1)-\theta H\}^3}{\left(1+\theta(\alpha_i-\beta_i+2)\right)^3}\right. \\
&\quad \left. -\frac{3(1-\theta)\{1+\theta(\alpha_i-\beta_i+1)-\theta H\}^2}{\left(1+\theta(\alpha_i-\beta_i+2)\right)^2}\right].
\end{aligned}$$

The above can be summarized as:

Theorem 7.1. The error of rational cubic function (3), for $f(x)\in C^3[x_0,x_n]$, in each subinterval $[x_i,x_{i+1}]$ is

$$\left|f(x)-S_i(x)\right| \le \frac{1}{2}\left\|f^{(3)}(\tau)\right\| h_i^3 c_i,$$

$$c_i = \max_{0\le\theta\le1} \omega(\alpha_i,\beta_i,\theta),$$

$$\omega(\alpha_i,\beta_i,\theta) = \begin{cases} \max \omega_1(\alpha_i,\beta_i,\theta), & 0\le\theta\le\theta^*, \quad 1-H>0, \\ \max \omega_2(\alpha_i,\beta_i,\theta), & 0\le\theta\le\theta^*, \quad 1-H<0, \\ \max \omega_3(\alpha_i,\beta_i,\theta), & \theta^*\le\theta\le1, \quad 1-H>0, \\ \max \omega_4(\alpha_i,\beta_i,\theta), & \theta^*\le\theta\le1, \quad 1-H<0. \end{cases}$$

Remark 7.2. For equal values of parameters $(\alpha_i=\beta_i)$ the rational cubic function (3) reduces to standard cubic Hermite. Thus the optimal error coefficient c_i for cubic Hermite can be obtained by substituting $\alpha_i=\beta_i$ in Theorem 5.1.

$$\omega_1(\theta) = \frac{8\theta^2(1-\theta)^3}{3(3-2\theta)^2}, \qquad 0\le\theta\le\tfrac{1}{2};$$

$$\omega_2(\theta) = \frac{8\theta^3(1-\theta)^2}{3(1+2\theta)^2}, \qquad \tfrac{1}{2} \le \theta \le 1 .$$

For standard cubic Hermite $c_i = \frac{1}{96}$.

8. Conclusion

In this study a two parameter family of C^1 rational cubic spline function is developed. The parameters have a direct geometric interpretation. The effect of parameters on the graphical display of data is demonstrated in Figures 1-4. Constraints are developed on one of the parameters to preserve the positive, monotone, convex and constrained data. The other parameter can assume any positive real value to visualize the shape preserving curve data. The order of approximation is investigated and is $O\left(h_i^3\right)$.

The data visualization schemes developed in this paper have constraints on one of the parameters to visualize for shape preserving curve data resulting less computational cost than the already developed schemes (see Hussain and Hussain (2007), Hussain and Sarfraz (2008), (2009), Sarfraz, Butt and Hussain (2001), Sarfraz (2003)), where more than one parameters were constrained to preserve the shape of data resulting increase in computational cost.

Unlike (Schmidt and Hess (1988)), the schemes developed in this paper are applicable to both data and data with derivatives. In (Lamberti and Manni (2001)), the step length was used as parameter for data visualization while the schemes developed in this paper do not constraint step length.

References

1. Brodlie, K. W. and Butt, S. (1991). Preserving convexity using piecewise cubic interpolation, Computers and Graphics, 15(1), 15-23.
2. Butt, S. and Brodlie, K. W. (1993). Preserving positivity using piecewise cubic interpolation, Computers and Graphics, 17(1), 55-64.
3. Dejdumrong, N. and Tongtar, S. (2007). The generation of G^1 cubic Bézier curve, fitting for Thai consonant contour, Geometic Modeling and Imaging – New Advances, Sarfraz, M., and Banissi, E., (Eds.) ISBN: 0-7695-2901-1, IEEE Computer Society, USA, 48 – 53.
4. Duan, Q., Zhang, H., Zhang, Y. and Twizell, E. H. (2007). Error estimation of a kind of rational spline, Journal of Computational and Applied Mathematics, 200(1), 1-11.
5. Fahr, R. D. and Kallay, M. (1992). Monotone linear rational spline interpolation, Computer Aided Geometric Design, 9, 313-319.
6. Goodman, T. N. T., Ong, B. H. and Unsworth, K. (1991). Constrained interpolation using rational cubic splines, Proceedings of NURBS for Curve and Surface Design, G. Farin (eds), 59-74.

7. Goodman, T. N. T. (2002). Shape preserving interpolation by curves, Proceeding of Algorithms for Approximation IV, J. Levesley, I. J. Anderson and J. C. Mason(eds.), University of Huddersfeld, 24-35.

8. Gregory, J. A. and Sarfraz, M. (1990). A rational cubic spline with tension, Computer Aided Geometric Design, 7(1-4), 1-13.

9. Hussain, M. Z. and Hussain, M. (2007). Visualization of data preserving monotonicity, Journal of Applied Mathematics and Computation, 190, 1353-1364.

10. Hussain, M. Z. and Sarfraz, M. (2008). Positivity-preserving interpolation of positive data by rational cubics, Journal of Computational and Applied Mathematics, 218(2), 446-458.

11. Hussain, M. Z. and Sarfraz, M. (2009). Monotone piecewise rational cubic interpolation, International Journal of Computer Mathematics, 86(3), 423-430.

12. Kvasov, B. I. (2000). Algorithms for shape preserving local approximation with automatic selection of tension parameters, Computer Aided Geometric Design, 17, 17-37.

13. Lamberti, P. and Manni, C. (2001). Shape-preserving C^2 functional interpolation via parametric cubics, Numerical Algorithms, 28, 229-254.

14. Sarfraz, M., Butt, S. and Hussain, M. Z. (2001). Visualization of shaped data by a rational cubic spline interpolation, Computers and Graphics, 25(5), 833-845.

15. Sarfraz, M. (2003). A rational cubic spline for the visualization of monotonic data: an alternate approach, Computers and Graphics, 27, 107–121.

16. Schmidt, J. W. and Hess, W. (1988). Positivity of cubic polynomial on intervals and positive spline interpolation, BIT, 28, 340-352.

17. Schultz, M. H. (1973). Spline Analysis, Prentice-Hall, Englewood Cliffs, New Jersey.

18. Yahaya, S. H., Hussain, M. Z. and Ali, J. M. (2006). Visualization of scientific data by a Bézier like quartic interpolation, Proceedings of the 2nd IMT-GT Regional Conference on Mathematics, Statistics and Applications, Universiti Sains Malaysia, Penang, June 13-15, 1-12.

19. Habib, Z. and Sakai, M. (2008). Transition between concentric or tangent circles with a single segment of G^2 PH quintic curve, Computer Aided Geometric Design, 25(4-5), 247-257.

20. http://www.analogzone.com/nett1108.pdf.